Some Peculiarities of Propagation and Reflection of Subsurface and Surface Waves in Solids

A. BAEV, P. PROKHORENKO, M. ASADCHAYA
Institute of Applied Physics, Minsk, Belarus

Abstract. New distinctive features of propagation of subsurface waves (*SW*) - longitudinal (SL) and transverse vertically polarized (*STV*) waves - in solids of different geometry have been studied experimentally. The peculiarities of formation of an acoustical field in an object with a projection have been revealed as a function of a curvature radius of a fillet transition, a wave frequency (1–4 MHz) and a probe type. The problems on the *SL* propagation in bodies with a cylindrical and two-face contact surface are considered, as well as the dependences of the amplitude attenuation of the *SL* mode as a function of a plate waveguide thickness are obtained. The studies of the *SL* reflection from the interface of media with different mixed boundary conditions have been performed.

Introduction

Subsurface longitudinal (*SL*) and vertically polarized transverse (*STV)* waves are excited at critical angles of incidence β_i of an ultrasonic beam, and propagate in solids along the surface (waveguide)

$$\beta_i = \arcsin(C_1/C_{2p}),$$

where C_1 and C_{2p} are ultrasonic velocities in the layers of contacting materials; index $p \equiv \{L, T\}$ refer to the wave mode used [1, 2].

Firstly, group of scientists [3 – 5], and some later - the others [5 – 7] has obtained significant experimental and theoretical data on excitation and propagation of *SL* waves in steel, which are important for development methods and instruments for ultrasonic flaw detection. So, these laboratory findings, as a rule, have been devoted to the study of only *SLW*-modes, obtained in simplified experimental conditions, where mode excitations and propagation's have been in solids with free and plane waveguide surfaces. Taking into account the wide possibilities from the previous type of wave application and real output problems, we began to study the laws of *SLW* and *STW* mode excitation and propagation in the solids of different geometric and boundary conditions at the interface surface [8 - 9].

Note, that a considerable number of objects subjected to ultrasonic flaw detection have projections and adjacent to them surface sections with a negative curvature radius: shafts of different equipment, welds, etc. In such a situation, a flaw zone is located near the projection or in the volume of the latter, and there is difficult to detect flaws. There are also the problems on the *SW* application for ultrasonic testing of the bodies with only cylindrical and two-face contact surface as well as of a plate form. Below are the experimental results on the peculiarities of formation of an acoustical field of subsurface waves in objects of the

above geometry have been studied. We also consider the problem of SW reflection from interface with mixed conditions.

1. Experimental method

Experimental techniques are clarified in the corresponding figures. Units of a standard acoustic flaw detector have been used as a source and amplifier of the probe signal. The signal's amplitude was measured by comparing it to the reference signal of a signal generator displayed on an oscilloscope screen. External synchronization, delay, and sweep of the signal were provided and its time characteristics were measured using an И2-26 device. Undetected probe signals 0f the belt form were used in the study, enabling an increase, owing to a specific feature of the equipment operation, in the accuracy of the measuring system. The directivity characteristic of the source of ultrasonic vibrations in the incidence plane $\Phi(\alpha)$ was determined using well-known recommendations [2, 4]. The transverse mode was detected by an electromagnetic-acoustic (EMA) probe. The width of the solenoid's winding determines the dimensions of the zone where vibrations can be detected; in the case considered, it is 0.0015 m. The localized high-strength field in the zone of E MA detection was created by closing the magnetic flux from the pole of a Sm-Co magnet with a steel plate whose front face contacts the solenoid's coils through a thin insulating plate. A 2-mm-wide and 10-mm-long normal piezoelectric probe was used as a detector of longitudinal vibrations.

2. Results and discussion

2.1. Propagation of subsurface waves in objects with projection

The results of most interest and importance for practice are presented in Figs.1-3 and describe the specific features of formation of a radiation field of *STV* probes with a mode $\Phi(\alpha)$ depending on the probe (position) coordinate along the x axis and the fillet transition radius R. As directly follows from the experimental data, at $R \leftarrows R/\lambda_R<10$ the dependences of $\Phi(\alpha)$ (or Φ on z) have two characteristic maxima P_{RT} and P_{ST}, a relationship between which $\varepsilon_{rt} = P_{RT}/P_{ST}$ is the function of both R' and x. In this case, the coordinate z_{rt} of the maximum P_{RT} lies above the coordinate z_{st} of the maximum P_{ST} . Note that the value and the angular position of the radiation field maximum P_{ST} is practically the same as in the case of no projection. The quantity P_{RT} can considerably change (by 10 dB and more) when the above parameters R' and x are varied and its coordinate can lie above or below the plane of the contact surface $z=0$.

To explain these experimental results, the fact that the *RW* mode is transformed into the transverse volumetric mode has been taken into account. The preliminary studies have shown that this mode is comparable in value with the principal one. Therefore, additional study has been made of the specific features of passing and transforming the surface waves at the above-mentioned objects. Consider the situation when an acoustical beam of the wedge falls as the second critical angle onto the interface of media, thus exciting in the object the principal *STV* mode and its accompanying Rayleigh mode, whose wavelengths are λ_t and λ_R , respectively. Passing through a curvilinear surface $b \le x \le b+R$, the latter re-radiates elastic waves into the solid, whose considerable amount of energy is transformed into the second mode [2, 10]. I.e., the curvilinear surface section in the vicinity of the fillet transition can be considered as the secondary source of *STV* waves. In this case, the

coefficient of energy conversion of the Rayleigh mode into the transverse one depends on a dimensionless fillet radius $R \leftrightarrows R/\lambda$ and can be presented in the form:

$$K_{RT} = W_{RT}/W_R = 1 - K_p - K_{ref} - K_0 ,$$

where K_p and K_{ref} are the energy transmission and reflection at the fillet transition with respect to energy, respectively; K_0 is the coefficient of the energy transformation into other modes. It is obvious that at $R \leftrightarrows R/\lambda >> 1$ $K_{RT} \to 0$. It is very difficult to obtain K_{RT} from calculations, as this requires an experimental approach. Note that K_{RT} and also "the effective aperture" of this source of waves and its directivity diagram of Φ_{RT} must not practically depend on the position (coordinate) of the probe. At the same time, in virtue of a weak disagreement and at small shifts, the Rayleigh wave amplitude will also vary slightly. The field of the primary *STV* (volumetric) mode radiated directly by the probe will undergo more essential changes in the projection volume as far as it moves from the projection.

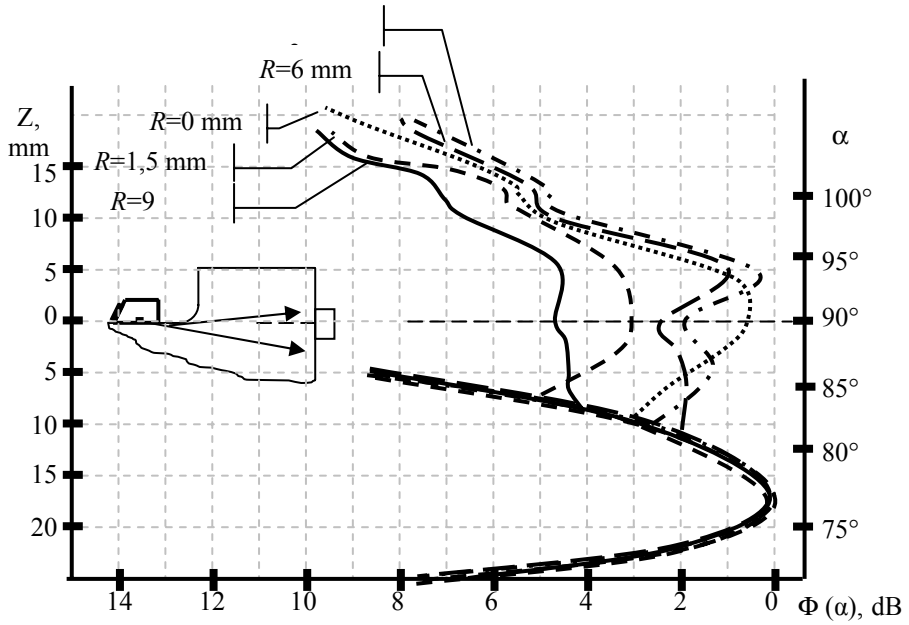

Fig.1.
Acoustical field of *STV* probe vs. radius of the fillet transition.

From the preliminary analysis and the above experimental data it can be concluded that the acoustical field in the considered region (projection volume) is formed by two coherent sources, whose amplitude is determined by geometrical parameters (R and x) and the velocity difference of the transverse C_T and Rayleigh C_R waves. Estimate the quantity $\Delta\Psi_{SR}$ - the phase over-run difference of the *ST* mode ($\Psi_{ST)}$ and the Rayleigh mode (Ψ_R). To do this, draw from the point of the probe index a circle with a radius $r_0 = l\text{-}b\text{-}R$ and estimate $\Delta\Psi_{SR}$ in covering a path l: from the point of the probe index to the fillet transition:

$$\Delta\Psi_{SR} = \Delta\Psi_1 + \Psi_{ST} - \Psi_R + \Psi_{RA}$$

where $\Delta\Psi_1$ is a possible phase shift at simultaneous excitation of the *ST* and *RW* modes; $\Psi_{ST} - \Psi_R = 2\pi\nu r_0 (C_T^{-1} - C_R^{-1})$; $\Psi_{RA} \approx 2\pi\nu\, k_{RA}\, \varphi R/C$; k_{RA} - some coefficient is lesser <1.

As the preliminary numerical estimations for a considerable number cases show, when $R \leq (1 \div 2)\lambda$, it is possible to neglect the phase shift Ψ_{Ra} that causes the pulse phase "delay" and amplitude variation when the wave is passing over the section of the curvilinear surface). Figs. 2-3 illustrate the essential influence of the phase shift $\Delta\Psi_{SR}$ on the acoustical field formed in the projection when transmitting probe changes its position. It is interesting that having chosen an optimum value of $\Delta\Psi_{SR}$ by varying the wave frequency

and the probe position, it becomes possible to increase the radiation field directivity. As seen, a change in the phase shift between primary and secondary radiation sources by the value ~π can be accompanied by a very significant change in the maximum amplitude ratio of the radiation field, ε (ΔP_{RT}), of the probe.

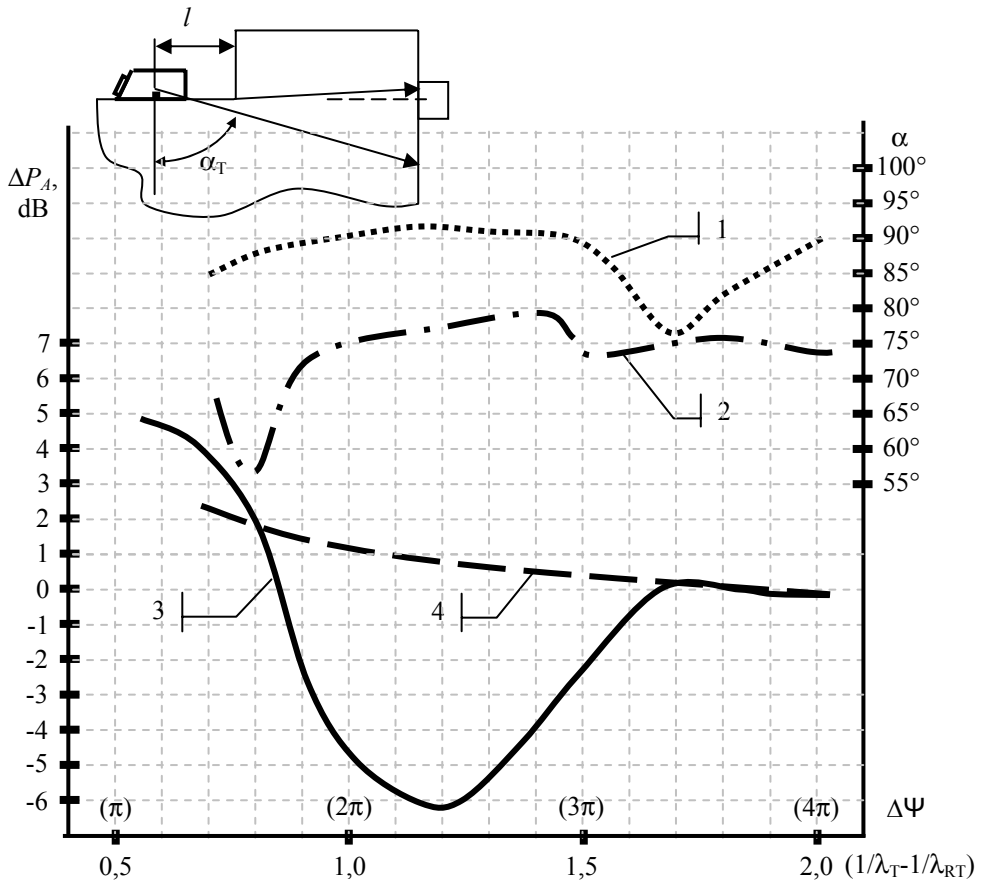

Fig.2.
Characteristic dependencies of the *STV* probe's acoustical field against its position *l*: 1, 2 – angles α of P_A maximums; 3 - ΔP,dB = $(P_{AR})_{max}$ - $(P_T)_{max}$; 4 – protrusion absent.

Consider the influence of the fillet transition on a field to be formed. Fig.4. shows, as the absolute quantity *R** is increased, the transmitting coefficientt K_{RT} for Rayleigh waves passing through a semi-cylindrical groove decreases. Apparently, the decrease in the coefficient K_{RT} causes the energy of a surface wave to transform into the one of a transverse mode. However, in this case, the transverse size of the surface section increases, radiating the second mode or the so-called "effective aperture" of the second radiator, which naturally should narrow the directivity diagram of the second *STV* source. It is important to pay attention to the fact that in the real situation, the sizes of considered objects (waveguides) are finite and the duration of a probing signal during a time t_{tr} is limited by a number of oscillations $n \approx 4 \div 5$ during $t_{tr} \approx n\nu^{-1}$. Therefore, the interaction of acoustical fields of the two above-mentioned sources (due to interference) is possible only when the phase difference of the two aforementioned up to the detection point does not exceed some characteristic value $\Delta\vartheta$.

It should be noted, that of independent significance are the results on the transformation effect $RW \rightarrow STV$. So, if $R' \ll 1$, then the maximum of the *SVT* radiation field is located somewhat below and is the nearly the same in frequency range (1 – 4) MHz. The

characteristic width $\Phi(\alpha)$ taken at a level of 3dB decreases by a factor of ~1.7 over the mentioned frequency range.

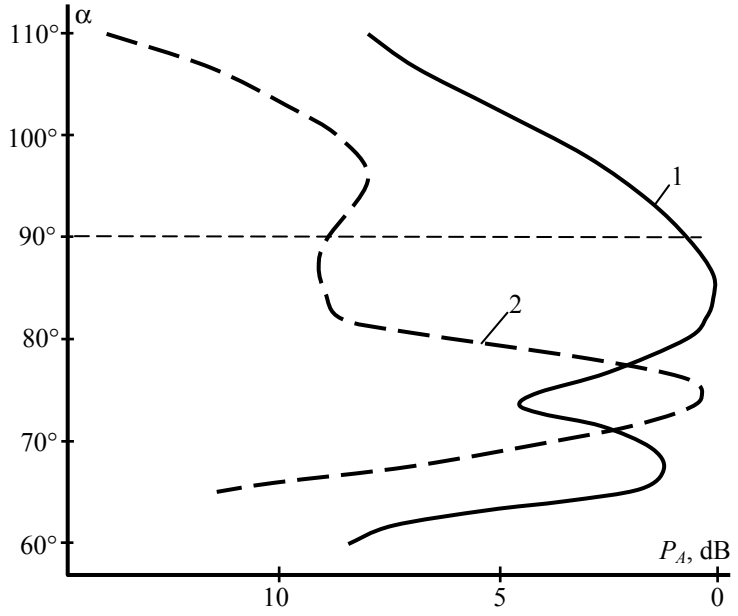

Fig.3.
Acoustical field of *STV* probe with operating frequency 1 MHz (1) and 1,85 MHz (2).

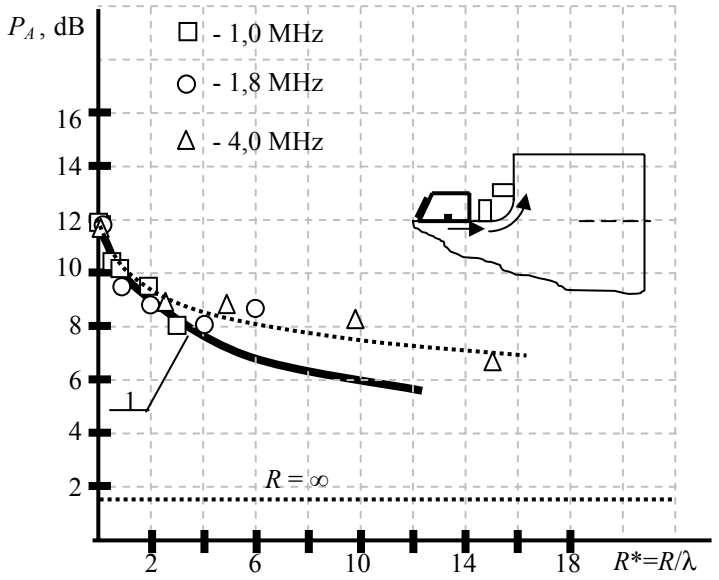

Fig.4.
Amplitude P_A of Rayleigh wave transmitted through curvilinear surface (1) and maximum of *STV* amplitude, transformed at the fillet transition (2).

And we found that longitudinal wave are to be appear too with amplitude of 25 – 30 dB lesser than the transformed *STV* mode is. Proceeding from the conducted investigations it can be concluded that by varying the signal frequency and the distance up to the fillet transition, the directivity of the transmitting probe radiation field of shear subsurface waves can be corrected. In a number of cases, when the high coefficient of transformation of a surface wave into the *STV* mode is taken into account, the application of surface wave

transformation into *STV* mode can be recommended for flaw detection. Yet, the following fact should be taken into consideration that if the fillet transition zone is controlled in "the duet regime", then the acoustical beam will somewhat deviate at the fillet transition boundary. This is caused by the way that the supersonic oscillation velocity of the surface mode differs from the transverse mode by ~8%.

2.2. SL waves in objects with cylindrical and two-face surfaces

The *SL* wave propagation in bodies with a cylindrical surface (R≤0) and a two-face surface have some specific features illustrated in Fig.5. Unlike the known investigations [9], the present study considers the dependencies P_A against the acoustical base when the probes is moving along the cylindrical surface generatrix. In this case, the receiving probe is 2.5 mm in size in the incidence plane and there occurs local receiving of just the surface *SL* mode that attenuates with distance much stronger than the volume one [10]. When objects with a two-face surface are being studied, the probe moves perpendicular to the line of face convergence.

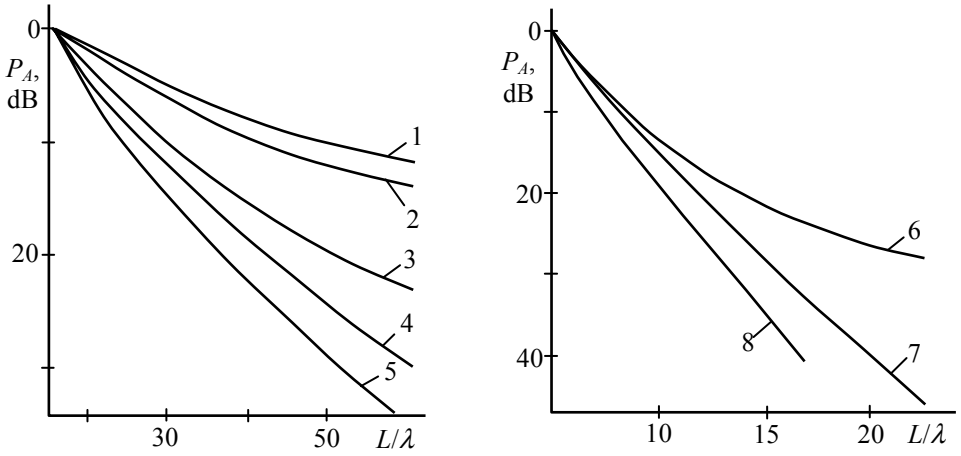

Fig.5.
Normalized dependencies $P_A(L/\lambda)$ of *SL* waves in objects with two-side surface (1-5) and cylindrical surface (6-8): θ, rad = 5/6 π (1); 11/12 π (2); π (3); 13/12 π (4); 7/6 π (5); λ_l/R = 0 (6); -0,04 (7); -0,08 (8).

It should be emphasized that there is some similarity of the obtained dependences of the wave amplitudes on the distance between the probes, which at $R<0$ (cylindrical surface) and the face angle $\varphi<\pi$ attenuate with distance much stronger than in the case of a plane object. So, it is found that when φ is varied over the range $\pi \div 5/6\pi$, the power of wave attenuation with the distance L is equal to $m \approx 2.38 - 2.6$ (symmetric position) or 2.43 (asymmetric). At the same time, when the angle between faces (probe working surfaces) $\varphi = \pi \div 7/6\pi$, $m \approx 1–1.2$ (symmetric position) and 1.69–1.47 (asymmetric), respectively. Note that if the SL mode propagation occurs along the cylindrical contact surface, then over the dimensionless curvature parameter range $\varepsilon=\lambda_l/R=(0\div-0.08)$ the power m takes values $m \cong 2\div5.1$. In this case, the maximum admissible acoustical base of sonic tests decreases up to $L/\lambda \cong 20$. Note, that in a number of cases, when acoustical processes are being modeled, because of difficulties in creating necessary conditions of input-reception it is possible to use bodies with a two-face surface instead of cylindrical ones.

2.3. SW wave propagation in waveguides of finite thickness

One of the important SW wave applications is associated with measuring a sonic velocity in bodies of finite size, which very often requires tuning out measurements from the noise background created by the modes re-reflected from the waveguide wall. Consider the case when the transmitter and the receiver operating in the through transmission regime are mounted at he base surface with the thickness h *(or* $h' = h/\lambda_l$ *)*. Using the ray acoustics principles, determine the conditions, at which there is no influence (superposition) of the signal reflected from the waveguide wall upon the one used for measuring an *SL* or *STV* mode pulse. These conditions can be applied for obtaining the nth "pure oscillation" in the pulse, and for the mentioned cases these are of the following form:

$$h' = \frac{h}{\lambda_t} > \varepsilon^* = \frac{h^*}{\lambda_t} = \sqrt{\frac{n^2}{4} + \frac{n}{2}\frac{L}{\lambda_t}} \quad (SL\ mode); \qquad \varepsilon^* = \frac{h^*}{\lambda_l} = \frac{\sqrt{4n^2 + 8n\frac{L}{\lambda_t} + 3\left(\frac{L}{\lambda_t}\right)^2}}{m+1} \quad (STV\ mode)$$

where m is the number of the longitudinal wave pulse reflected in the waveguide.

As seen, the critical value of the plate waveguide thickness h^* depends on the wavelength of a faster (longitudinal) mode, the period number of oscillations in the pulse, the acoustical base length. In the case of the *STV* mode use, the waveguide thickness must be chosen as twice as large. The presented in Fig.6 experimental curves for the wave attenuation $P(L')$ are the monotonically decreasing functions and at some $L' < (L^*)'$ do not depend on the plate thickness. But for $L' > (L^*)'$ These curves diverge from the similar curve for a semi-infinite body. It should be noted that the experimental value of L^* are somewhat larger than the predicted ones. So, e.g., at $h' = 4.66$ and 1.69 the experimental data $(L^*)' \approx 50$ and 10, and the predicted data are 45 and 5, respectively. Nevertheless, above expressions obtained by a rather simple method can be used for estimating the conditions, at which ultrasonic measurements can be made using *STV* and *SL* waves in plate waveguides. (It should be mentioned that at some $h' < h^{*\prime}$,weakly damping modes with a pronounced pulse shape are excited in plate waveguides where the s_o mode is the most fast and its velocity is somewhat smaller than the *SW* mode velocity [10]).

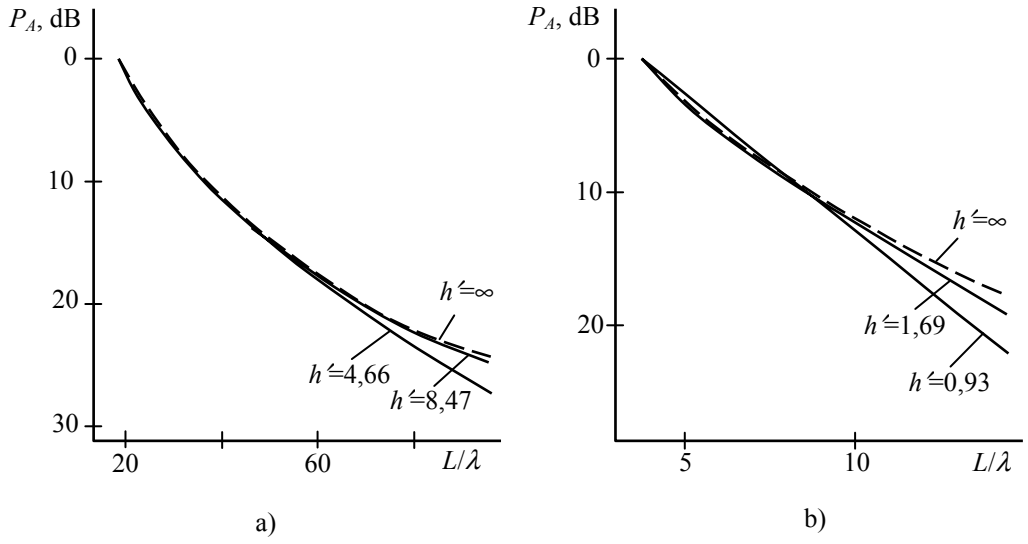

Fig.6.
Normalized experimental dependencies $P_A(L/\lambda)$ for steel plates of different thickness for ν =1 MHz (a) and 5 MHz (b).

2.4. Reflection from the interface of media with mixed boundary conditions

Some peculiarities of the *SL* when applied to ultrasonic control are revealed. As shown in [11], there are certain conditions for input-reception of ordinary volume waves, at which a very high sensitivity of control over the adhesion quality of materials is attained. Use of SW waves is advisable for control of adhesion of material, whose surface is mainly perpendicular to the contact surface of object. Below is modeled the situation when at the sound-reflecting surface two boundary conditions are simultaneously created with respect to the components of stresses (σ_{in}, $\sigma_{i\tau}$) and shifts (ξ_{in}, $\xi_{i\tau}$): free ($\sigma_{in}=\sigma_{i\tau}=0$) and sleep ($\sigma_{1n}=\sigma_{2n}$, $\sigma_{1\tau}=\sigma_{2\tau}=0$, $\xi_{in}=\xi_{2n}$). The procedure of experimental studies is explained in Fig.7, where an object is subjected to sounding by subsurface waves according to "the duet scheme". To model the sleep boundary, the end of a metal (base) sample is equipped with "a sample-reflector", that is shifted with constant clamping along the x or y coordinate. (The surfaces of samples contact each other through a layer of contact lubricant no less than 5μm in thickness). When "the sample-reflector" is shifted, the straight line (*LBC*) separating the reflection regions with different boundary conditions is shifted too. Thus, the acoustical field of a reflected acoustical beam can be presented in the form of the superposition of fields of imaginary coherent sources with different amplitude and phase. Depending on the *LBC* position, the value of a reflected signal on the receiving probe can essentially vary (up to 20 dB and more). This is also seen in the case when effective amplitudes of signals reflected from different surface sections are the same. When the phase difference $\Delta\varphi\approx\pi$ between the latter is present, there occurs the most pronounced transformation of a field of reflected waves and the maximum control sensitivity is reached. This can be easily shown theoretically and supported experimentally. Note that when the line *LBC* moves along x, due to interference there occurs something like splitting of the main blade of the directivity diagram expansion mainly in the horizontal plane. If LBC moves along y, then this process occurs mainly in the vertical plane. Thus, the conducted studies have revealed that longitudinal subsurface waves can be used for implementing the high-sensitive method for control of adhesion of materials that is based on the principles of creating optimal conditions for superposition of fields of imaginary coherent sources [11].

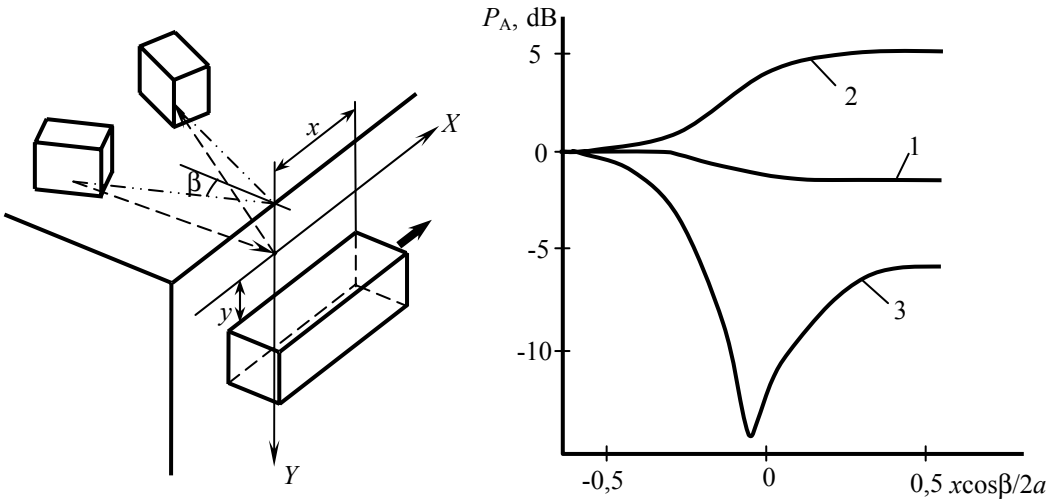

Fig.7.
Amplitude P_A of *SL* waves reflected from interface with sleep-free boundary conditions against of *x* and *y* coordinate of the specimen-reflector: $y/2a''$= 0,5 (1); 0 (2); -1,2 (3).

3. Conclusions

The physical model of forming the acoustical radiation field $\Phi(\alpha)$ of *STV* wave transmitting probe in bodies with a step projection is developed. It is based on the representation of $\Phi(\alpha)$ as a superposition of the fields of two coherent sources: the principal mode and the secondary mode transformed at the fillet transition from the accompanying Rayleigh wave. When the latter is transformed, the longitudinal volume mode is generated, which is by 25 – 30 dB smaller than the amplitude. It is found that at a sufficiently small radius of the fillet transition ($R/\lambda_R<<1$), the maxima of the radiation field of the secondary *STV* mode over the frequency range $\nu=1\div4$ MHz practically coincide with the measuring error and is located somewhat below the plane of the contact surface. The characteristic width $\Phi(\alpha)$ taken at a level of 3dB decreases by a factor of ~1.7 over the mentioned frequency range.

From the obtained results on the propagation of *SL* waves in objects with cylindrical ($-\varepsilon=\lambda_R/R=(0\div0.08)$) and two-face ($5\pi/6\leq\varphi\leq7\pi/6$) surfaces as well as in plates the maximum permissible values of acoustical bases are determined in ultrasonic measurements using the through transmission method.

The conducted studies have revealed that longitudinal subsurface waves can be used for implementing the high-sensitive method for control of adhesion of materials that is based on the principles of creating optimal conditions for superposition of fields of imaginary coherent sources.

References

[1] Brekhovskikh, L. M., *Waves in layered media*. London, New York:Academic Press, 1960, 511 p.

[2] Krautkramer J., Krautkramer G., *Ultrasonic material evaluation*, Metallurgy, Moscow, 1991, p.722.

[3] Ermolov, I. N., Razygraev, N. P. and Shcherbinskii V. G., *Sov. J. of NDT*, 1978, Vol. 14, pp. 27-33.

[4] Ermolov, I. N., Razygraev, N. P. and Shcherbinskii V. G., *Sov. J. of NDT*, 1978, Vol. 14, pp. 953-957.

[5] Ermolov, I. N., Razygraev, N. P. and Shcherbinskii V. G., *Sov. J. of NDT*, 1979, Vol. 15, pp.28-30.

[6] Gytis, M. B., Himunin, A. D., *Sov. J. of NDT*, 1991, N 914, p. 52.

[7] Nikiforov, L.A. and Kharitonov, A.V., *Defectoskopiya*, 1981, no.6, pp. 80-85.

[8] Bayev, A.R. and Asadchaya, M.V., *Russian Journal of Nondestructive Testing*, 2005, Vol. 41, no. 9, pp. 567-576.

[9] Bayev, A.R. and Asadchaya, M.V., *Russian Journal of Nondestructive Testing*, 2005, Vol. 41, no. 9, pp. 577-585.

[10] Viktorov, I. A., *Rayleigh and Lamb waves*, New York: Plenum Press, 1967, 403 p.

[11] Baev, A., Abstracts of Int. Conf.: Ecology and waves. – Belarus, Minsk, 1993. p.95.